IOPscience iopscience.iop.org

Home Search Collections Journals About Contact us My IOPscience

Exact mapping of the d_{x2-y2} Cooper-pair wavefunction onto the spin fluctuations in cuprates: the Fermi surface as a driver for 'high T_c' superconductivity

This article has been downloaded from IOPscience. Please scroll down to see the full text article.

2009 J. Phys.: Condens. Matter 21 012201

(http://iopscience.iop.org/0953-8984/21/1/012201)

View the table of contents for this issue, or go to the journal homepage for more

Download details:
IP Address: 129.169.10.56
The article was downloaded on 11/09/2010 at 19:48

Please note that terms and conditions apply.

IOP FTC

IOP PUBLISHING JOURNAL OF PHYSICS: CONDENSED MATTER

J. Phys.: Condens. Matter **21** (2009) 012201 (6pp) doi:10.1088/0953-8984/21/1/012201

FAST TRACK COMMUNICATION

Exact mapping of the $d_{x^2-y^2}$ Cooper-pair wavefunction onto the spin fluctuations in cuprates: the Fermi surface as a driver for 'high T_c' superconductivity

Ross D McDonald, Neil Harrison and John Singleton

National High Magnetic Field Laboratory, TA-35, MS-E536, Los Alamos National Laboratory, Los Alamos, NM 87545, USA

E-mail: jsingle@lanl.gov

Received 22 May 2008, in final form 6 November 2008
Published 1 December 2008
Online at stacks.iop.org/JPhysCM/21/012201

Abstract

We propose that the extraordinarily high superconducting transition temperatures in the cuprates are driven by an exact mapping of the $d_{x^2-y^2}$ Cooper-pair wavefunction onto the incommensurate spin fluctuations observed in neutron-scattering experiments. This is manifested in the direct correspondence between the inverse of the incommensurability factor δ seen in inelastic neutron-scattering experiments and the measured superconducting coherence length ξ_0. Strikingly, the relationship between ξ_0 and δ is valid for both $La_{2-x}Sr_xCuO_4$ and $YBa_2Cu_3O_{7-x}$, suggesting a common mechanism for superconductivity across the entire hole-doped cuprate family. Using data from recent quantum-oscillation experiments in the cuprates, we propose that the fluctuations responsible for superconductivity are driven by a Fermi-surface instability. On the basis of these findings, one can specify the optimal characteristics of a solid that will exhibit 'high T_c' superconductivity.

(Some figures in this article are in colour only in the electronic version)

Although there is strong experimental evidence that the 'high-T_c' cuprates possess a superconducting order parameter with $d_{x^2-y^2}$ symmetry [1], the mechanism for superconductivity remains a matter for debate [2]. In this paper, we point out that the experimentally-determined Cooper-pair wavefunction in the cuprates maps directly onto the spin-fluctuation distribution responsible for the antiferromagnetic peaks measured in inelastic neutron scattering [2–7]. This strongly suggests that the superconductivity in the cuprates is mediated by the spin fluctuations. In this context, it should be noted that the fluctuations (figure 1(a)) have characteristic maximum energies ~500 K [2–7], a plausible energy scale for the values of $T_c \lesssim 100$ K observed in the cuprates [2].

Recent measurements of magnetic quantum oscillations in the underdoped cuprates [8–12] suggest the likely cause of the fluctuations. These experiments reveal a number (1–3) of small Fermi-surface pockets (quantum-oscillation frequencies $\lesssim$2000 T), likely to result from the incommensurate nesting of the predicted (large) hole Fermi surface [11–14]. The nesting vectors inferred from the topology of the small Fermi pockets [11] are consistent with the wavevectors of the spin fluctuations determined in the neutron-scattering measurements [2–7]. This strongly suggests that the fluctuations are driven by Fermi-surface instabilities [11], and that the development of their dispersion with increasing hole doping p [2–7] reflects the evolution of the underlying Fermi-surface topology.

We begin by considering the $d_{x^2-y^2}$ Cooper-pair wavefunction. Most treatments of superconductivity consider the state as a condensate [15–19]; in such a picture, it is natural to treat the Cooper-pair wavefunction in k-space. However, we are interested in the similarity of the spatial distribution of

 © 2009 IOP Publishing Ltd Printed in the UK

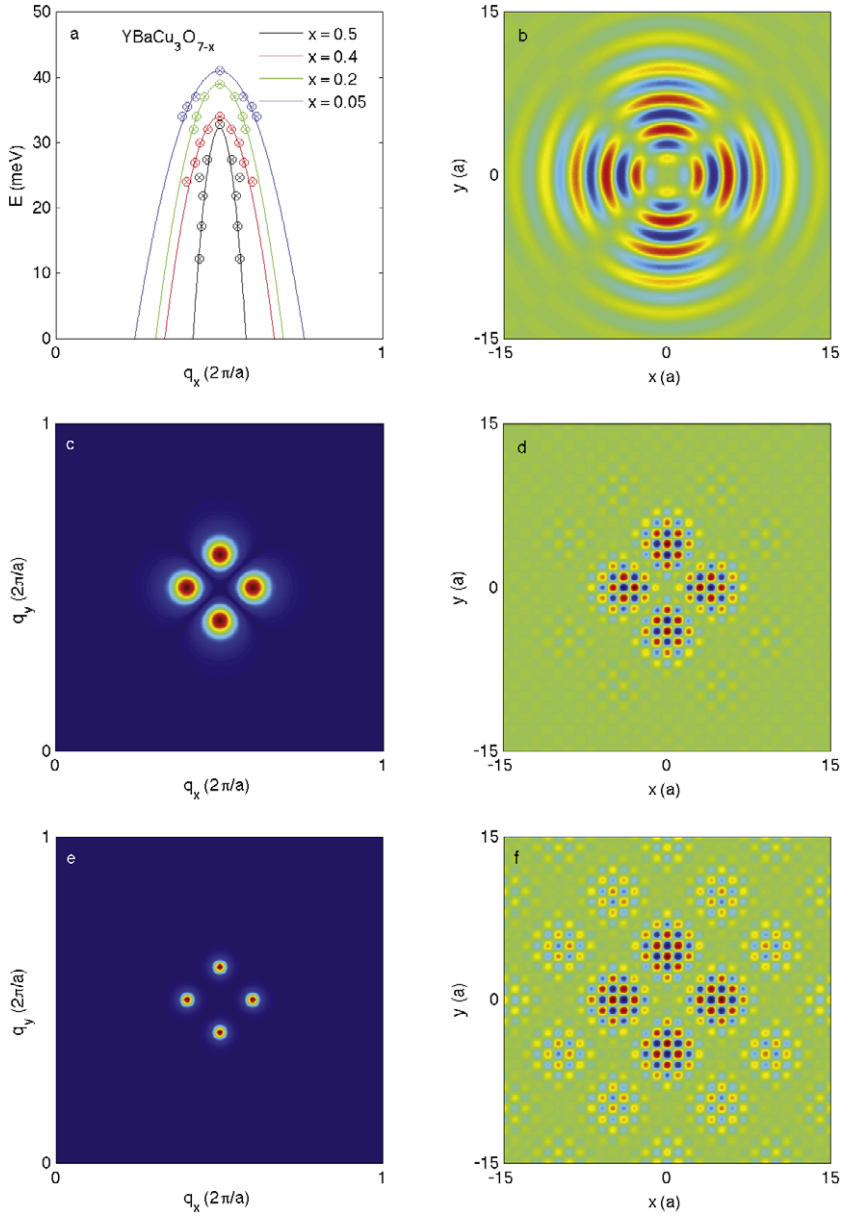

Figure 1. (a) Energy (E) versus q_x for several $YBa_2Cu_3O_{7-x}$ compositions (points) [5, 6], with fits to equation (2) to obtain extrapolated values of δ at $E = 2$ meV (curves). (b) Contour plot of d-wave Cooper-pair wavefunction in two-dimensions (equation (1)); we assume a Fermi wavevector $k_F = \pi/\sqrt{2}a$ where a is the lattice parameter, while $p = 0.1$, for which we select $\xi_0 = 27$ Å from table 1. (c), (e) Simulation of the incommensurate neutron-scattering peaks obtained by Fourier transforming equation (3); δ and ξ correspond to $p = 0.1$ (table 1). (d), (f) Real-space spin-fluctuation map corresponding to the set of four incommensurate peaks in (b), also for $p = 0.1$ (see table 1). The middle row ((c), (d)) corresponds to the lower bound of correlation length, the bottom row ((e), (f)) the upper bound (table 1). We consider the simple case where $s_{\mathbf{Q}}$ is the same for all $\mathbf{Q}$.

spin fluctuations and the Cooper pairs, and so we consider the form of the two-dimensional $d_{x^2-y^2}$ Cooper-pair wavefunction in real space [1, 19]:

$$\psi(\mathbf{r}) \propto \cos(rk_F)(x^2 - y^2)e^{-3r/\xi_0}. \quad (1)$$

Here $r = \sqrt{x^2 + y^2}$ is the cylindrical polar radius, x and y are corresponding Cartesian coordinates, k_F is the Fermi wavevector [8, 9] and ξ_0 is the superconducting coherence length. Figure 1(b) shows a contour plot of $\psi(\mathbf{r})$; the known diagonal nodal regions [1, 18] are clearly visible. In such a plot, the lengthscale over which $\psi(\mathbf{r})$ is non-negligible is defined by ξ_0 (equation (1)); coherence lengths ξ_0 derived from magnetoresistance and other data [21, 22] are given in table 1 for several cuprates with different composition and hole doping p. As we will later compare these data to inelastic neutron-scattering results, some interpolation has been used to obtain values for the same p and composition as the samples used in the neutron experiments.

We now consider the similarity of the $d_{x^2-y^2}$ Cooper-pair wavefunction (figure 1(b), equation (1)) to the real-space topology of the incommensurate antiferromagnetic fluctuations seen in inelastic neutron scattering [2–7]. Low-energy

Table 1. Parameters for various cuprate superconductors, including hole doping p. For $La_{2-x}Sr_xCuO_4$, δ values measured at neutron transfer energies of $E \approx 2$–3 meV are taken from [4, 7]. For $YBa_2Cu_3O_{7-x}$, δ values at the equivalent energy are taken from plots such as figure 2(a) using data from [5, 6]. Correlation lengths ξ are taken from [3, 4] while BCS coherence lengths ξ_0 are taken from [21, 22], occasionally requiring interpolation between adjacent compositions for precise doping matches to δ. For compounds in which more than one estimate of ξ has been reported, the range of values obtained is given.

Compound	p	δ	ξ (Å)	ξ_0 (Å)	T_c (K)
$La_{1.94}Sr_{0.06}CuO_4$	0.06	0.05	17	56	13
$La_{1.925}Sr_{0.075}CuO_4$	0.075	0.07	14	44	33
$La_{1.92}Sr_{0.08}CuO_4$	0.08	0.08	11	36	24
$YBa_2Cu_3O_{6.5}$	0.082	0.078	9	33	59
$YBa_2Cu_3O_{6.6}$	0.097	0.16	7.5	22	62.7
$La_{1.9}Sr_{0.1}CuO_4$	0.10	0.10	12–33	27	29
$YBa_2Cu_3O_{6.8}$	0.123	0.18	4	24	71.5
$La_{1.88}Sr_{0.12}CuO_4$	0.12	0.115	17	25	33.5
$La_{1.86}Sr_{0.14}CuO_4$	0.14	0.1225	12	22	35
$La_{1.85}Sr_{0.15}CuO_4$	0.15	0.1225	14–50	20	38
$YBa_2Cu_3O_{6.95}$	0.152	0.24	3.3	12	93
$La_{1.82}Sr_{0.18}CuO_4$	0.18	0.13	9–40	19	35.5
$La_{1.75}Sr_{0.25}CuO_4$	0.25	0.125	8	28	15
$La_{1.73}Sr_{0.27}CuO_4$	0.27	0.1	10	34	7

inelastic neutron-scattering data for both $La_{2-x}Sr_xCuO_4$ [4, 7] and $YBa_2Cu_3O_{7-x}$ [5, 6] follow an approximately inverted parabolic form

$$E(\mathbf{q}) = E_0\left(1 - \frac{a^2(\mathbf{q}-\mathbf{Q}_0)^2}{\pi^2\delta^2}\right), \qquad (2)$$

where a is the in-plane lattice parameter and E_0 is a doping-dependent energy scale [2–6]; some examples are shown in figure 1(a). Here, δ depends on the composition and hole doping p of the cuprate involved [2, 3, 20]; some values are given in table 1. As $E \rightarrow 0$, the brightest scattering intensity typically appears at a cluster of four incommensurate peaks at $\mathbf{Q} = (\pm\pi/a, \pm(1 \pm 2\delta)\pi/a)$ and $(\pm(1 \pm 2\delta)\pi/a, \pm\pi/a)$ [2–7]; a simulation is shown in the positive q_x, positive q_y quadrant of two-dimensional k-space in figure 1(c). The form of the scattering peaks in figures 1(c) and 1(e) is already very suggestive of the $d_{x^2-y^2}$ wavefunction in figure 1(b); to make a quantitative comparison, however, we require a real-space representation of the corresponding spin fluctuations.

A simple model of spin fluctuations that can produce the observed incommensurate scattering peaks is a sinusoidal variation of the staggered moment modulated by an exponential damping factor; the latter term represents the fact that the antiferromagnetic fluctuations possess a finite correlation length ξ [3, 20]. The spatially-varying moment is thus

$$s(\mathbf{r}, t) = \sum_{\mathbf{Q}} s_{\mathbf{Q}} \exp\left(-\frac{r}{\xi} + i\omega t\right) \cos(\mathbf{Q}\cdot(\mathbf{r}-\mathbf{r}_0)), \qquad (3)$$

where ω is the angular frequency of the fluctuations, $\mathbf{r}_0 = (\pm d, 0)$ or $(0, \pm d)$ with $d = a/2\delta$, and the sum in $\mathbf{Q}$ runs over the values given above. Whilst the experimental values of d are well constrained by the positions of scattering peaks in the neutron data, the extraction of ξ is more dependent on the method used to fit the scattering *lineshape*; hence, quite a wide spread of ξ values is given in the literature (see e.g. [3, 4]). In what follows, we shall use both the lowest and the highest reported values of ξ in our simulations to show that the main conclusion of this paper is unaffected by the choice of ξ; it is the lengthscale d, rather than ξ, that is more important in determining the form of the spatial distribution of the spin fluctuations.

Figures 1(c) and (e) show Fourier transforms of equation (3) for the lowest and highest reported values of ξ. These simulations reproduce the general form of the experimental neutron data [2–7] very well. Note that the choice of $\mathbf{r}_0$ is quite critical; any other value would give significant intensity at $\mathbf{q} = \mathbf{Q}_0$, at variance with the experimental spectra. This is an important point, to which we will return.

Figures 1(d) and (f) show time-averaged contour plots of equation (3), again for the lowest and highest reported values of ξ. The similarity between the spin-fluctuation distributions and the $d_{x^2-y^2}$ wavefunction (figure 1(b)) is most marked: both show similar angular and radial distributions. Less obvious, but equally germane, is the phase of each function plotted. The choice of $\mathbf{r}_0$ necessary to reproduce the neutron data means that there is a π difference of phase between adjacent lobes of the spin-fluctuation distribution, exactly the same as the π difference in phase between adjacent lobes of the $d_{x^2-y^2}$ Cooper-pair wavefunction [1, 18].

Finally, we remark that d plays a very similar role in the spin-fluctuation spatial distribution to that of ξ_0 in the Cooper-pair wavefunction; via the oscillatory term in equation (3), d determines the lengthscales over which the spin-fluctuation magnitude is largest and over which it first falls to zero. By contrast, quite large variations in ξ are relatively unimportant; the positions of the maxima and minima in $s(\mathbf{r}, t)$ are little affected (compare figures 1(d) and (f)). In subsequent simulations we therefore use the mean ξ in cases where there is a spread in values.

Values of $d = a/2\delta$ may be deduced using the δ taken from inelastic neutron-scattering measurements shown in table 1. In the $La_{2-x}Ca_xCuO_4$ cuprates, the dispersion relationships (figure 1(b)) have been measured down to low energies, providing accurate values of δ [4]. However, there is a loss of intensity at lower-energy transfers in $YBa_2Cu_3O_{7-x}$, possibly because of their greater homogeneity [5, 6], necessitating a downward extrapolation of the dispersion curves to obtain δ in the limit $E \rightarrow 0$.

Having tabulated experimental values of δ and ξ_0 for various hole densities p (table 1), we can now plot the evolution with increasing p of the spatial distribution of the spin fluctuations (equation (3)) alongside the corresponding Cooper-pair wavefunction (equation (1)); figure 2 shows the result. At small values of p, the incommensurate neutron-scattering peaks occupy a small area of k-space [4–6]; the corresponding real-space spin-fluctuation distribution occupies a large area, as does the Cooper-pair wavefunction. As p increases, the incommensurate peaks spread out in k-space [4–6]; hence, the spin-fluctuation spatial distribution is

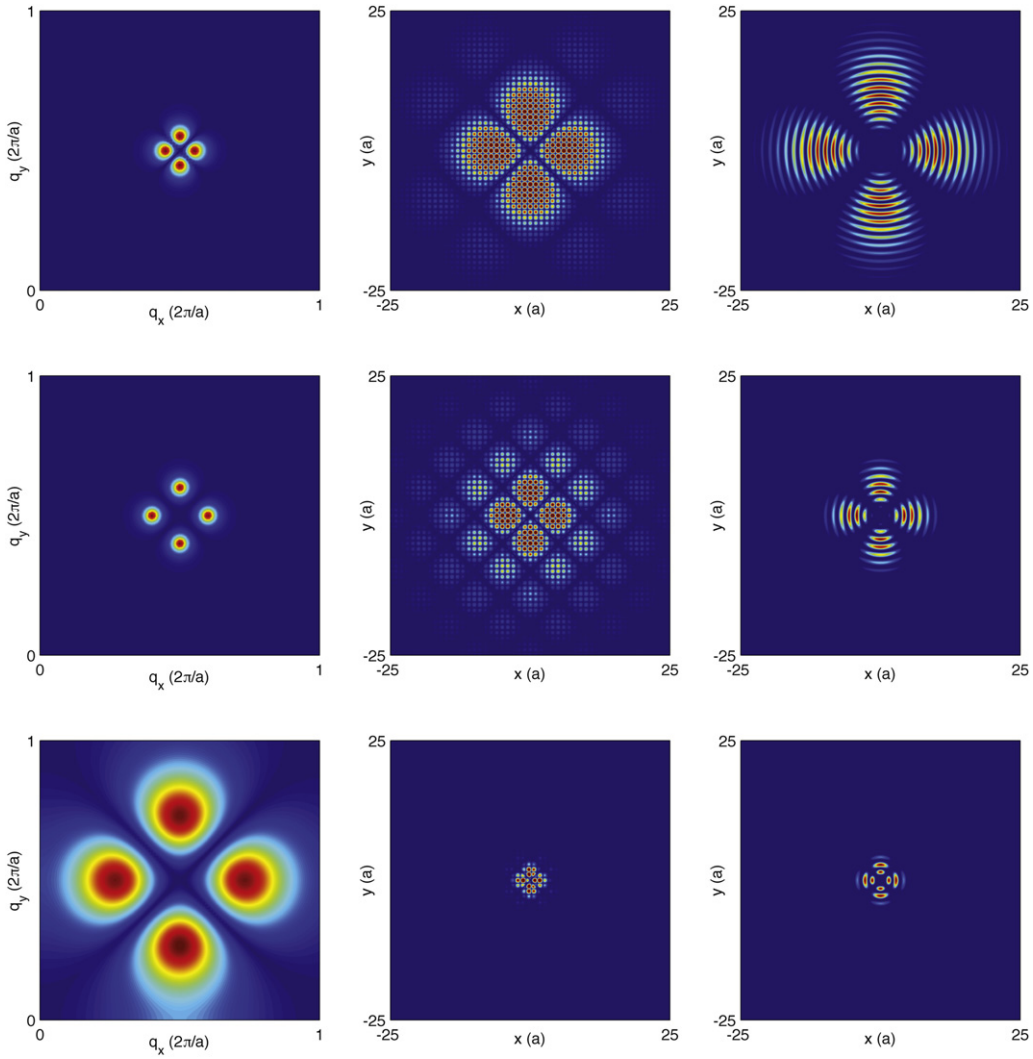

Figure 2. Comparisons of the spin-density amplitude and $d_{x^2-y^2}$ wavefunction at selected values of p. The first column shows plots of the incommensurate diffraction peaks obtained on re-Fourier transforming $s(\mathbf{r})$ calculated using equation (3) and the published values of δ and ξ listed in table 1. The second column shows the calculated $|s(\mathbf{r})|$ while the third column shows $\rho_c(\mathbf{r}) = |\Psi(\mathbf{r})|^2$ calculated according to the values of ξ_0 listed in table 1. Rows 1, 2 and 3 consecutively correspond to $p \approx 0.06$, 0.1 and 0.152. Note that where a range of ξ values are listed in table 1 the average is used.

compressed, as is the Cooper-pair wavefunction. Although the tabulated values of ξ_0 and δ (table 1) are deduced from completely independent experiments (the former from thermodynamic or transport data, the latter from neutron scattering), there is a very close match between the physical size of the $d_{x^2-y^2}$ Cooper-pair wavefunction and the spatial extent of the spin-fluctuation distribution.

The very similar spatial extent of the Cooper-pair wavefunction and the spin fluctuations strongly suggests a causal relationship between the two phenomena. Examination of equations (1) and (3) shows that the spin-fluctuation amplitude is largest at the vector locations $(\pm d, 0)$ and $(0, \pm d)$, whilst the $d_{x^2-y^2}$ Cooper-pair wavefunction has greatest probability amplitude at $(\pm\frac{2}{3}\xi_0, 0)$ and $(0, \pm\frac{2}{3}\xi_0)$. Therefore, if the spin fluctuations are responsible for the superconducting pairing, one would expect that

$$2\xi_0 = 3d, \tag{4}$$

independent of hole doping p. Figure 3(a), which plots experimental values of ξ_0 against d (from table 1), shows that this is in fact the case for *both* $La_{2-x}Sr_xCuO_4$ *and* $YBa_2Cu_3O_{7-x}$. Irrespective of doping and composition, the data for all materials lie close to the single straight line $2\xi_0 = 3d$ (equation (4)). This suggests that the same causal connection between the spin fluctuations and superconductivity holds for *all* of the cuprates.

Before turning to the origin of the incommensurate scattering peaks in the neutron data [2–7, 11], it is worth re-iterating the factors that lead us to propose a causal relationship (or one might say spatial resonance) between superconductivity and antiferromagnetic fluctuations in the cuprates.

(i) On setting $\mathbf{r}_0 = (\pm d, 0)$ or $(0, \pm d)$ where $d = a/2\delta$, the π difference in phase between the adjacent 'spin clusters' in figure 1(d) is aligned with the π difference in

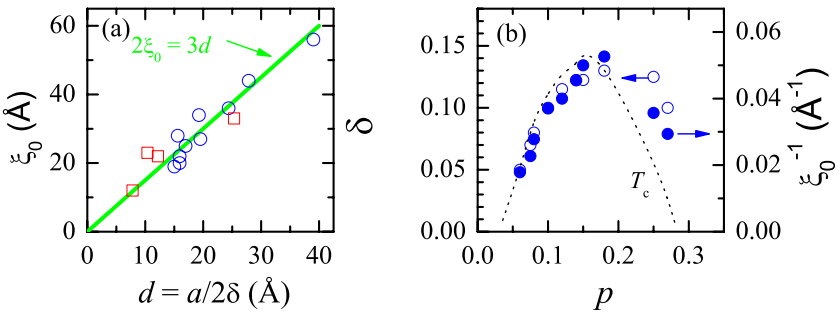

Figure 3. (a) The approximately linear correspondence between $d = a/2\delta$ and ξ_0 for $La_{2-x}Sr_xCuO_4$ (circles) and $YBa_2Cu_3O_{7-x}$ (squares). The line represents the ratio $2\xi_0 = 3d$ (equation (4)). (b) Plot showing δ and ξ_0^{-1} in $La_{2-x}Sr_xCuO_4$ exhibiting a maximum versus p in a similar fashion to T_c (scaled for comparison), though T_c falls more rapidly with p beyond optimal doping.

phase between adjacent lobes of the $d_{x^2-y^2}$ Cooper-pair wavefunction (figure 1(b)). The spin fluctuations are therefore 'in phase' with the Cooper-pair wavefunction.

(ii) Independent of our choice of wavefunction, there is a very direct correspondence between ξ_0, which determines the overall size of the Cooper pair, and δ, which quantifies the physical separation $d = a/2\delta$ between adjacent clusters of spins in real space (figures 2 and 3). As mentioned above, this results in the $2\xi_0 = 3d$ slope (equation (4)) in figure 3(a).

While there are certainly systematic and random errors in the methods used to extract ξ_0 values [21, 22], they are consistent in $La_{2-x}Sr_xCuO_4$ with estimates obtained from strong-coupling variants of the BCS formulae $\xi_0 = \hbar v_F/\pi\Psi_0$ and $2\Psi_0/k_BT_c \approx 4$–5, where Ψ_0 is the $T = 0$ order parameter [16, 17], using typical Fermi velocities $v_F \approx 6$–8×10^4 m s^{-1} determined from quantum-oscillation experiments on $YBa_2Cu_4O_8$ and $YBa_2Cu_3O_{6.5}$ [8–12]. This provides a natural explanation for the observed linear dependence of δ on T_c [4, 7]. A slightly stronger coupling $2\Psi_0/k_BT_c \approx 6$ is required for the $YBa_2Cu_3O_{7-x}$ series [5, 6].

Incommensurate diffraction peaks in metallic systems are almost always associated with Fermi-surface nesting, in which the periodicity of spin or change modulation is determined by the topology of the Fermi surface [23]. Whilst the tight-binding calculations of the cuprate Fermi surface usually give a single, large hole pocket [13, 14], the recent experimental observations of (multiple) small pockets in the underdoped cuprates [8, 9, 11, 12] supports the suggestion that some form of nesting occurs [11, 13, 14]. Added weight is given by the similarity of the incommensurate mode dispersion (figure 1(b)) to those observed in itinerant antiferromagnets such as Cr and $V_{2-x}O_3$ [24–26] (both above and below the Neél temperature).

In such a picture, the cuprate Fermi surface plays an increasingly important role as the hole doping p is increased. Thus, just as in $V_{2-x}O_3$ [24], large-moment antiferromagnetic insulator behaviour in the cuprates eventually gives way to small-moment incommensurate itinerant antiferromagnetic behaviour as the system becomes more metallic [3, 14]. Consistent with itinerant magnetism, the orbitally-averaged Fermi velocity $v_F = \sqrt{2e\hbar F}/m^* \approx 8 \times 10^4$ m s^{-1}, where F is the Shubnikov–de Haas oscillation frequency, of the pockets in $YBa_2Cu_3O_{6.5}$ [8, 11] is comparable to the mode velocity $v_0 = 2aE_r/\pi\hbar\delta \approx 14 \times 10^4$ m s^{-1} (at $E = 0$) that one obtains fitting equation (2) to the E-versus-$\mathbf{q}$ data points obtained from inelastic neutron-scattering experiments on the same sample composition [6][1] (figure 1(b)). As p increases toward optimum doping, E_0 in figure 1(a) also increases [2, 3, 20], providing a suitable characteristic energy scale (~10 s meV, i.e. ~100 s of kelvin) for T_c [2].

In conventional BCS superconductors, the quasi-particle interactions that result in pairing are via charge coupling to acoustic phonon modes [16, 17]. The incommensurate spin fluctuations have a dispersion relationship (figure 1(a)) analogous to that of the acoustic phonons (i.e. approximately linear as $E \rightarrow 0$, saturating at a maximum energy that defines the energy scale of T_c). However, in contrast to the acoustic phonons, which have $E = 0$ at the Brillouin-zone centre, $E = 0$ in the antiferromagnetic-fluctuation dispersion relationships occurs at finite q, leading to the coupling between the lengthscales ξ_0 and d (figures 1(a) and 3). No such lengthscale phenomenology occurs in conventional s-wave superconductors, where the $q \rightarrow 0$ phonons mediate the pairing mechanism.

The remaining ingredient in the problem is therefore a coupling mechanism between the spin fluctuations and the charge inherent in the Cooper pair. This is found in the large onsite correlation energy U, which inhibits double occupancy of spins or holes [27]. Consequently, local variations in the density of holes $\Delta\rho_h$ and spin-density amplitude Δs are expected to be subject to the relation

$$\Delta\rho_h \propto -\Delta|s|. \tag{5}$$

Pairing mechanisms involving this behaviour have been considered both in the weak (small Hubbard U) [28] and strong (large Hubbard U) [29] coupling limits, although typically in conjunction with long-range antiferromagnetic order. However, there is no reason to suspect that such mechanisms will not apply in regimes where the antiferromagnetism is strongly fluctuating [3]. Therefore, because of the reciprocity relationship (equation (5)), the slowly varying modulation of the spin-fluctuation intensity should be accompanied by

[1] Ideally, v_0 should be compared with the Fermi velocity of the unreconstructed Fermi surface, which is expected to be somewhat higher owing to its larger cross-section in k-space [13, 14].

a concomitant charge modulation $\bar{\rho}_h(\mathbf{r}) \propto -|\bar{s}(\mathbf{r})|$. The very similar form of $\rho_h(\mathbf{r}) \propto -|s(\mathbf{r})|$ in the second column of figure 2 to $\rho_c \propto |\Psi(\mathbf{r})|^2$ in the third column of figure 2 therefore provides direct evidence for a 'spatial charge commensurability' between the Cooper-pair wavefunction and incommensurate spin fluctuations.

Qualitatively, the Cooper pairs in this work are spatially compact near optimum doping (figure 3), resembling the strong-coupling spin-bipolarons of Mott and Alexandrov [27, 29]. Away from optimum doping,they become spatially extended, like a weak-coupling $d_{x^2-y^2}$ variant of the 'spin bags' proposed by Schrieffer *et al* [28]. The difference between these pictures is that the fluctuations mediating the superconductivity in the present proposal are characteristic of a system on the brink of long-range order, rather than an established antiferromagnet.

In summary, based on measurements including Fermi-surface studies [8–12], neutron-scattering data [2–6] and resistivity experiments [21, 22], we propose that the unusually high superconducting transitions in the cuprates are driven by an exact mapping of the incommensurate spin fluctuations onto the $d_{x^2-y^2}$ Cooper-pair wavefunction. The spin fluctuations are driven by the Fermi-surface topology, which is prone to nesting [11, 13, 14]; they couple to the itinerant holes via the strong onsite Coulomb correlation energy U, which prohibits double occupancy of spins or holes [27]. The maximum energy of the fluctuations (∼100s of kelvin [2, 3, 20]) gives an appropriate energy scale for the superconducting T_c. Based on these findings, one can specify the features necessary for a solid to exhibit 'high T_c' superconductivity; (i) the material should be quasi-two-dimensional, with the conducting layers exhibiting four-fold symmetry (to ensure that fluctuations are optimally configured to a d-wave order parameter); (ii) the material should have a Fermi-surface topology susceptible to nesting, so as to produce antiferromagnetic fluctuations with a large degree of incommensurability δ; (iii) however, the electron–phonon coupling should be moderate, to prevent formation of stripe or charge–density-wave-like phenomena that compete with superconductivity [30]; in other oxides, the larger electron–phonon coupling dominates, preventing superconductivity [31].

We are grateful to Ed Yelland, Roger Cowley, Wei Bao, Sasha Balatsky, Bill Hayes and Bill Buyers for stimulating discussions. This work is supported by the US Department of Energy (DoE) BES programme 'Science in 100 T'. NHMFL is funded by the National Science Foundation, DoE and the State of Florida.

References

[1] Tsuei C C and Kirtley J R 2000 *Rev. Mod. Phys.* **72** 696
[2] Schrieffer J R and Brooks J S (ed) 2007 *High-Temperature Superconductivity Theory and Experiment* (Berlin: Springer)
[3] Kampf A P 1994 *Phys. Rep.* **249** 219
[4] Yamada K *et al* 1998 *Phys. Rev.* B **57** 6165
[5] Dai P *et al* 2001 *Phys. Rev.* B **63** 054525
[6] Stock C *et al* 2005 *Phys. Rev.* B **71** 024522
[7] Wakimoto S *et al* 2004 *Phys. Rev. Lett.* **92** 217004
[8] Doiron-Leyraud N *et al* 2007 *Nature* **447** 565
[9] Yelland E A *et al* 2008 *Phys. Rev. Lett.* **100** 047003
[10] Bangura A F *et al* 2008 *Phys. Rev. Lett.* **100** 047004
[11] Sebastian S E *et al* 2008 *Nature* **454** 200
[12] Singleton J *et al* 2008 *Physica* B at press
[13] Julian S R and Norman M 2007 *Nature* **447** 537
[14] Harrison N *et al* 2007 *Phys. Rev. Lett.* **99** 206406
[15] Cooper L N 1956 *Phys. Rev.* **104** 1189
[16] Bardeen J, Cooper L N and Schrieffer J R 1957 *Phys. Rev.* **108** 1175
[17] Tinkham M 1975 *Introduction to Superconductivity* (New York: McGraw-Hill)
[18] Lee G S 1994 *Phys. Rev.* B **49** 3616
[19] Kadin A M 2007 *J. Supercond. Nov. Magn.* **20** 285
[20] Monthoux P, Balatsky A V and Pines D 1992 *Phys. Rev.* B **46** 14830
[21] Ando Y and Segawa K 2002 *Phys. Rev. Lett.* **88** 167005
[22] Wen H H *et al* 2003 *Europhys. Lett.* **64** 790–6
[23] Grüner G 1994 *Rev. Mod. Phys.* **66** 1
[24] Bao W *et al* 1996 *Phys. Rev.* B **54** R3726
[25] Stockert O *et al* 2001 *J. Magn. Magn. Mater.* **226** 505
[26] Endoh Y and Böni P 2006 *J. Phys. Soc. Japan* **75** 111002
[27] Zhang F C and Rice T M 1988 *Phys. Rev.* B **37** 3759
[28] Schrieffer J R, Wen X-G and Zhang S-C 1988 *Phys. Rev. Lett.* **60** 944-7
[29] Mott N F 1991 *Phil. Mag. Lett.* **64** 211
Alexandrov A S 1998 *Physica* C **305** 46
[30] Tranquada J M *et al* 2004 *Nature* **429** 534
Tranquada J M *et al* 1996 *Phys. Rev.* B **54** 7489
[31] Milward G C *et al* 2005 *Nature* **433** 607